Fast Beam Alignment Via True Time Delay Frequency Dependent Beamforming Using Fixed and Variable Length Tests

Christoph Jans, Wolfgang Rave, and Gerhard Fettweis
Vodafone Chair Mobile Communications Systems, Technische Universität Dresden, Germany
Email: {christoph.jans, wolfgang.rave, gerhard.fettweis}@tu-dresden.de

***Abstract*—In this work, we present a time efficient solution to the initial beam alignment/acquisition of a hybrid beamforming millimeter wave communication system. Our proposal is based on adding a frequency dependent beamforming device at the transmitter which is capable of simultaneously testing all spatial angles and, therefore, any set of possible beamformers from an analog codebook. Such a device employed outperforms any kind of consecutive beamformer testing, e.g., exhaustive search, in terms of testing overhead and receive power loss after beamforming. To further increase the time efficiency, a variable length testing technique in combination with the frequency dependent beamformer is described, which is adaptive to any signal to noise ratio or varying channel condition. Especially in the low signal to noise ratio regime, an overall speed-up can be achieved. The described radar-like solution to the initial beam alignment problem may act as an enabler for mmWave communication in fast-varying and challenging environments.**

I. Introduction

A never ending demand for higher data rates in the order of $100\,\mathrm{Gbit\,s^{-1}}$ for various applications in the field of self-driving cars, virtual reality, or augmented reality [1], [2] can only be satisfied by enabling data communication at frequencies in the millimeter wavelength (mmWave) regime and above, where large chunks of unlicensed bandwidth are available. Unfortunately, communications at these frequencies suffer from large path losses which need to be compensated. Therefore, highly directional antenna arrays at the transmitter and/or receiver side are employed. However, directional antenna arrays on both ends, at user equipment (UE) and base station (BS), need to be aligned such that receive powers are maximized and energy and/or data can successfully be transmitted. Challenges like a short coherence time due to movement of transmitters/receivers/scatterers, e.g., persons or vehicles in the environment [1], demand a time-efficient beam alignment procedure to enable mmWave communication. Implementing beamforming digitally is often intractable, due to increased hardware complexity (larger number of radio-frequency (RF) chains) and increased signalling overhead for estimating a high-dimensional channel state matrix. Therefore, we propose a hybrid beamforming system with a focus on the analog beam alignment in this work. In such a system, a distinct set of analog beamformers from a given codebook is tested. Suitable beamformer pairs are found by iterating through the complete codebook and testing each pair for maximum beamforming gain or receive power.

A common method which tests all beamformers consecutively is called *exhaustive search* (ES) and can be seen as a brute force approach that is guaranteed to find the optimal solution to the underlying problem [3]. However, this is very ineffective as it wastes a lot of time on testing non-promising beam patterns. Moreover, exhaustive search used in downlink beam-training often inherently assumes some kind of frame/time synchronization prior to beam alignment, which is often neglected in literature, but needs to be established [4]. On first glance, the results in [4], [5] seem to relax the requirement for accurate time synchronization, using uplink beam training, where each UE transmits a unique sequence during a random access phase which are then received and filtered by the BS. However, in this approach a BS needs to distinguish between several UEs solely based on their pilot sequences and test beamformers to maximize the receive power sequence per UE. Orchestrating several users and enhancing such a scheme to handle multi-user scenarios is limited by pilot sequence design and finding sequences with good auto/cross correlation properties. Otherwise separation of all UEs in code/time/frequency and/or space might fail.

In contrast, we would like to stress the fact that our proposed *frequency dependent beamforming* (FDB) is perfectly suitable for downlink training and does not rely on prior time synchronization between UEs and BS at all. In this work, every UE can listen to the pilot signal broadcast of the BS and decide on the best beamformer to be used. FDB, which is referred to as *frequency scanning arrays* [6], can outperform state-of-the art exhaustive search techniques such as [3], [7]. One might argue that FDB just trades time-resources for frequency-resources to test all possible directions. However, in mmWave communications (and above) we can typically assume a frequency flat channel [8] and, therefore, testing beamformers at only a fraction of available the system bandwidth is sufficient. Improvements w.r.t. shorter beam alignment phases, as proposed in this work, are vital to pave the road towards multi-gigabit links at sub-terahertz frequencies. Especially given that the number of beams will be very large at high carrier frequencies, due to the large number of antenna elements required to compensate the small area efficiency per antenna element.

Our prior investigations were limited to line-of-sight (LOS) scenarios and are in this work extended to multi-path channels [8]. Furthermore, we improve on the variable length testing [3] procedure and propose a downlink single-carrier training scheme, which is fully capable of testing an analog orthogonal codebook and does not use an orthogonal frequency division multiplexing (OFDM) solution as in [7], [9].

II. System Model

We assume downlink transmission from a BS with a uniform linear array (ULA) of M antenna elements. For simplicity, we

assume single-antenna UEs. Nevertheless, our results are not limited to single-antenna UEs and are extendable to antenna arrays on both sides. In the transmission environment, we assume a few scatterers $l \in 1, \ldots, L$ modelled according to the mmWave channel model in [8], where each scatterer is defined by three parameters: 1) α_l - the attenuation/path gain, 2) ϕ_l - the angle of departure (AoD), and 3) τ_l - the random time delay between BS and UE. Therefore, any received bandpass signal is a superposition of delayed copies of an up-converted baseband signal $s(t)$. To be specific, the wideband bandpass pilot signal $s^{BP}(t-\tau_{m,l}) = Re\{s^{BB}(t-\tau_{m,l})\, e^{2j\pi f_c(t-\tau_{m,l})}\}$ is delayed by $\tau_{m,l}$ which captures the timing delay between antenna element m and the UE for path l. Thus, we can define the following input-output relation in the bandpass regime $r_l^{BP}(t) = \sum_{m=0}^{M-1} s^{BP}(t-\tau_{m,l})$ for the contribution of path l and after down-conversion to baseband we obtain

$$r_l(t) = \alpha_l \sum_{m=0}^{M-1} s(t-\tau_{m,l})\, e^{-j2\pi f_c \tau_{m,l}}, \tag{1}$$

with carrier frequency f_c. Assuming a stationary process, where the pilot sequence $s(t)$ is periodically repeated and received by the UE, Fourier transformation yields the following description in frequency domain

$$R_l(f) = \alpha_l S(f) \sum_{m=0}^{M-1} e^{-j2\pi(f_c+f)\tau_{m,l}}. \tag{2}$$

Each mth timing delay $\tau_{m,l}$ can be split into three parts

$$\tau_{m,l} = \tau_{m,l}^p + \tau_m^s + \tau_l, \tag{3}$$

where $\tau_{m,l}^p$ is an element of the propagation delay vector

$$\boldsymbol{\tau}_l^p = \left(\begin{bmatrix} 0 & \ldots & M-1 \end{bmatrix} - \frac{M-1}{2} \right) \frac{d}{c} \sin\phi_l, \tag{4}$$

corresponding to the AoD ϕ_l w.r.t. to the phase center of the ULA with antenna element spacing d and c being the speed of light. The timing delays τ_m^s from vector $\boldsymbol{\tau}^s$ can be chosen *freely*, and model the true time delay of the beamforming at each antenna element m of the ULA. Last, the random time-of-arrival/flight delay τ_l specifies the delay between phase center of the BS antenna array and single antenna UE.

To achieve optimal energy transfer and, thus, perfect beam alignment, one needs to compensate the timing offsets in (4) by equalizing/delaying the pilot signal $s(t)$ per antenna element with adequate selection of τ_m^s. However, in hybrid beamforming the analog codebook is limited to a discrete set of predefined true time delays. As in [10], [11], we use true time delay steering vectors $\boldsymbol{\tau}_q^s = \frac{q}{Mf_c}[0, \ldots, M-1]^T$ of size M, where the complete set of $q \in 0, \ldots, M-1$ vectors forms a matrix

$$\mathbf{F}_{TTD}^{orth} = \frac{1}{f_c M} \begin{bmatrix} 0 \\ 1 \\ \vdots \\ M-1 \end{bmatrix} \begin{bmatrix} 0 & 1 & \ldots & M-1 \end{bmatrix}. \tag{5}$$

and creates an orthogonal analog beamformer codebook. Implementations in hardware for such an orthogonal codebook can be found in [12], [10], [11].

A. Exhaustive Search

Testing each beamformer $q \in [0, ..., M-1]$ of the analog codebook (5) one after the other is referred to as Exhaustive Search. By selecting the mth element of column q in $\mathbf{F}_{TTD}^{orth}$, we redefine the overall timing delay per path l and antenna element m as

$$\tau_{m,l}^{ES} = \{\boldsymbol{\tau}_l^p\}_m + \{\mathbf{F}_{TTD}^{orth}\}_{m,q} + \tau_l, \tag{6}$$

where τ_l is the random time delay.

We make the *narrowband* assumption for the ULA as described in more detail in [13]: as long as the transit time of a planar wave traveling along the array is shorter than the Nyquist sampling interval $T_s = 1/f_b$, where f_b is the signal bandwidth, $\max\{\boldsymbol{\tau}_l^p\} \ll T_s$, and $\max\{\{\mathbf{F}_{TTD}^{orth}\}_q\} \ll T_s$, we can use the following approximation for the receive signal under beam q:

$$r_{l,q}^{ES}(t) \approx \alpha_l \sum_{m=0}^{M-1} s(t-\tau_l)\, e^{-j2\pi f_c \tau_{m,l}^{ES}} \tag{7}$$

Replacing the sum of exponentials with the inner product between the array propagation vector corresponding to angle ϕ_l

$$\mathbf{a}_p^H(\phi_l) = \begin{bmatrix} e^{j2\pi f_c \frac{M-1}{2}\frac{d}{c}\sin\phi_l} & \ldots & e^{-j2\pi f_c \frac{M-1}{2}\frac{d}{c}\sin\phi_l} \end{bmatrix} \tag{8}$$

and the array steering vector

$$\mathbf{a}_{s,q}^{ES} = \begin{bmatrix} e^{-j2\pi q(0)/M} & \ldots & e^{-j2\pi q(M-1)/M} \end{bmatrix}^T, \tag{9}$$

we end up with

$$r_{l,q}^{ES}(t) = \alpha_l s(t-\tau_l)\, e^{-j2\pi f_c \tau_l} \mathbf{a}_p^H(\phi_l)\, \mathbf{a}_{s,q}^{ES}, \tag{10}$$

which is

$$R_{l,q}^{ES}(f) = \alpha_l S(f)\, e^{-j2\pi(f_c+f)\tau_l} \mathbf{a}_p^H(\phi_l)\, \mathbf{a}_{s,q}^{ES} \tag{11}$$

in frequency domain. The well-known beam patterns of an orthogonal codebook for a ULA are obtained by multiplying $\mathbf{a}_p^H(\phi)\, \mathbf{a}_{s,q}^{ES}$ with $\phi = [-\pi/2, \pi/2]$ and are shown in Fig. 1 for $M = 4$ orthogonal beams.

Sampling $r_{l,q}^{ES}(t)$ according to the Nyquist sampling theorem $kT_s = k/f_b$ and adding complex Gaussian random noise samples $z[k]$, we obtain the noisy sampled output signals per beamformer q and sample k

$$y_q^{ES}[k] := y_q^{ES}(kT_s) = \sum_l r_{l,q}^{ES}[k] + z[k]. \tag{12}$$

B. Frequency Dependent Beamforming

Instead of generating a discrete set of frequency independent beam patterns under the narrowband assumptions using the delays in (5), we now intentionally violate this assumption to create frequency dependent beams [9], [14]. This can be achieved by delaying the signal at antenna m of the transmit array by an integer multiple of the reciprocal of the signal bandwidth (i.e. the sampling interval T_s). Analogously, we redefine $\tau_{m,l}$ for FDB such that

$$\tau_{m,l}^{FDB} = \{\boldsymbol{\tau}_l^p\}_m + mT_s + \tau_l. \tag{13}$$

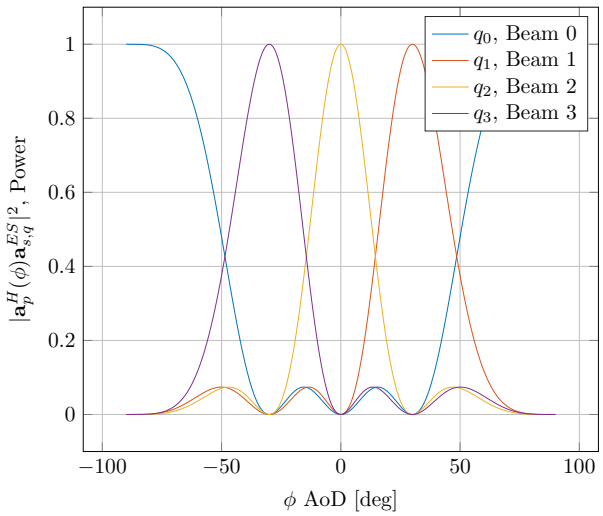

Fig. 1: Orthogonal beam patterns of ULA with $M = 4$, with $f_c = 100\,\text{GHz}$, $f_b = 1\,\text{GHz}$

Due to the large value of the time shift mT_s we cannot neglect it in $s\left(t - \tau_{m,l}^{FDB}\right)$. However, the smaller propagation delays with maximum value of $\max\{\boldsymbol{\tau}_l^p\} \ll T_s$, can be neglected and we approximate the receive signal for path l as

$$r_l^{FDB}(t) \approx \alpha_l \sum_{m=0}^{M-1} s(t - mTs - \tau_l)\, e^{-j2\pi f_c \tau_{m,l}^{FDB}} \quad (14)$$

or in frequency domain

$$R_l^{FDB}(f) \approx \alpha_l S(f) \sum_{m=0}^{M-1} e^{-j2\pi f(mTs+\tau_l)} e^{-2j\pi f_c \tau_{m,l}^{FDB}}. \quad (15)$$

Replacing the sum with the inner product between array propagation vector (8) and frequency *dependent* array steering vector

$$\mathbf{a}_s^{FDB}(f) = \left[e^{-j2\pi(f+f_c)0T_s} \ldots e^{-j2\pi(f+f_c)(M-1)T_s}\right]^T \quad (16)$$

we end up with the following spectrum for the received signal for path l

$$R_l^{FDB}(f) = \alpha_l S(f)\, e^{-j2\pi(f+f_c)\tau_l} \mathbf{a}_p^H(\phi)\, \mathbf{a}_s^{FDB}(f). \quad (17)$$

Sampling the spectrum $R_l^{FDB}(f)$ equidistantly with kf_s, where $f_s = f_b/K^{FDB}$ being the frequency resolution or fundamental frequency, and adding complex Gaussian noise samples $Z[k]$, we obtain the discrete representation of the spectrum

$$Y^{FDB}[k] := Y^{FDB}(kf_s) = \sum_l R_l^{FDB}[k] + Z[k] \quad (18)$$

based on noisy observations of $r_l^{FDB}(t)$, where

$$R_l^{FDB}[k] := \alpha_l S(kf_s)\, e^{-j2\pi(kf_s+f_c)\tau_l} \times \mathbf{a}_p^H(\phi)\, \mathbf{a}_s^{FDB}(kf_s) \quad (19)$$

and K^{FDB} is the total number of used sampled frequencies.

A corresponding time-domain representation can be found by taking the inverse Fourier transform $r_l^{FDB}(t) = \mathcal{F}^{-1}\{R_l^{FDB}(f)\}$ of (17) or in the discrete case the discrete inverse Fourier transform of $R_l^{FDB}[k]$.

III. Beam Alignment - Fixed Length Testing

We start the discussion about time-efficiency by explaining the beam alignment for a fixed length scenario. Fixed length testing means that a total number of samples is predefined and after collecting N samples, we decide in favor of the best beamformer from the analog codebook. Typically, N is designed for a given average expected SNR for all possible UEs in the field and, therefore, leads to suboptimal results for varying SNR values.

A. Exhaustive Search

As mentioned earlier, exhaustive search selects beamformer q and compares its receive power to all other $|Q| - 1$ beamformers in the analog codebook.

The detection method is based on cross-correlating the receive signal with the known sampled pilot sequence $s[k]$

$$\hat{x}_q^{ES}[k] = \sum_{u=0}^{K^{ES}-1} s^*[u]\, y_q^{ES}[u+k] \quad (20)$$

for all possible shifts u of the cyclically repeated pilot signal. The length of the pilot sequence is $K^{ES} = T^{ES}/T_s$ with T^{ES} being its period length. Summing up all magnitudes of $\left(\sum_k |\hat{x}_q^{ES}[k]|^2\right)^{\frac{1}{2}}$, its maximum

$$\hat{q}_{max} = \arg\max_{q \in Q} \sqrt{\sum_k \left|\hat{x}_q^{ES}[k]\right|^2} \quad (21)$$

defines the estimated beamformer to use after testing.

Replacing $y_q^{ES}[k]$ in (20) with the noise-free observation $\sum_l r_{l,q}^{ES}[k]$ and adapting (21) accordingly, we obtain x_q^{ES} and the optimal q_{max}. With x_q^{ES} and the optimal q_{max}, our performance measure is defined as the relative average loss of receive power, i.e., the ratio of receive power of the estimated maximum beamformer and the receive power of the noise-free maximum beamformer

$$\bar{l} = 1 - \mathrm{E}\left[\sqrt{\frac{\left(\sum_k |x_{\hat{q}_{max}}^{ES}[k]|^2\right)}{\left(\sum_k |x_{q_{max}}^{ES}[k]|^2\right)}}\right]. \quad (22)$$

This approach needs at least $|Q|K^{ES}$ samples and lasts $|Q|T^{ES}$ to decide for the best beamformer. So for a total number of observations N, the maximum pilot sequence length for exhaustive search to test all beamformers with the same number of observations is $K^{ES} = N/M = N/|Q|$.

B. Frequency Dependent Beamforming

From [15], we know that frequency dependent beamforming excites all AoDs simultaneously and each AoD is addressed by a certain frequency f of the total bandwidth. An OFDM-based pilot symbol with subcarrier frequencies [7], [9] exciting the spatial beam patterns (5) can test the complete analog codebook simultaneously in the frequency domain. However, repeating a linear chirp with period length MT_s, where we set $K^{FDB} = M$ so that the spectral representation of the receive signal has

the smallest possible value to determine the best beamformer in the codebook of (5) with lowest computation effort.

Such a periodic time domain signal is best explained by starting from the frequency domain representation, where all $k \in \left[-\frac{K^{FDB}}{2}, \ldots, \frac{K^{FDB}}{2}-1\right]$ discrete frequency samples (18), define the spectrum of the discrete receive signal

$$\mathbf{Y}^{FDB} = \sum_{l} \alpha_l \mathbf{a}_p^H(\phi_l)\, \mathbf{A}\mathbf{D}_l\mathbf{S} + \mathbf{Z} \tag{23}$$

of size $1 \times K^{FDB}$. Here,

$$\mathbf{A} = \left[\mathbf{a}_s^{FDB}\left(-\tfrac{K^{FDB}}{2} f_s\right) \quad \ldots \quad \mathbf{a}_s^{FDB}\left(\left(\tfrac{K^{FDB}}{2}-1\right) f_s\right)\right] \tag{24}$$

is the frequency dependent array steering matrix of size $M \times K^{FDB}$. The diagonal matrix

$$\mathbf{D}_l = \begin{bmatrix} e^{-j2\pi\left(-\frac{K^{FDB}}{2} f_s + f_c\right)\tau_l} & \ldots & 0 \\ \vdots & \ddots & \vdots \\ 0 & \ldots & e^{-j2\pi\left(\left(\frac{K^{FDB}}{2}-1\right) f_s + f_c\right)} \end{bmatrix} \tag{25}$$

of size $K^{FDB} \times K^{FDB}$ represents the random timing offset between BS and UE at the frequencies of interest, and the matrix of size $K^{FDB} \times K^{FDB}$

$$\mathbf{S} = \begin{bmatrix} S\left(-\frac{K^{FDB}}{2} f_s\right) & \ldots & 0 \\ \vdots & \ddots & \vdots \\ 0 & \ldots & S\left(\left(\frac{K^{FDB}}{2}-1\right) f_s\right) \end{bmatrix} \tag{26}$$

represents the spectrum of the pilot signal at the same frequencies. Finally, $\mathbf{Z}$ is a vector of random complex Gaussian noise samples of size $1 \times K^{FDB}$.

The corresponding periodically repeated discrete time domain representation is obtained by taking the inverse discrete Fourier Transform (iDFT). Therefore, we multiply (23) with iDFT-matrix $\mathcal{D}^H$ of size $K^{FDB} \times K^{FDB}$ from the right. This sequence is then repeated N/K^{FDB} times to match the total amount of observations as for the exhaustive search, and we obtain the vector

$$\mathbf{y}^{FDB} = \mathbf{x}^{FDB}\tilde{\mathbf{S}} + \mathbf{z} = \sum_{l} \alpha_l \mathbf{a}_p^H(\phi_l)\, \mathbf{A}\mathbf{D}_l\tilde{\mathbf{S}} + \mathbf{z} \tag{27}$$

with $\tilde{\mathbf{S}} = \left[\mathbf{S}\mathcal{D}^H, \ldots, \mathbf{S}\mathcal{D}^H\right]$ of size $K^{FDB} \times N$, where $\mathbf{S}\mathcal{D}^H$ of size $K^{FDB} \times K^{FDB}$ corresponds to one period of the training signal in time domain. The complex Gaussian random vector $\mathbf{z}$ of length N collects all time domain noise samples. Recalling that if we chose $f_s = \frac{f_b}{K}$, we equidistantly sample the spectrum and, thereby, probe with similar spatial beamformers at the same mainlobe directions as those in (5). In Fig. 2, the effect of repeating the matched pilot sequence of length $K^{FDB} = M$ is shown. First, one can see that by repeating $\mathbf{S}$, a discrete set of frequencies excites the FDB device and a distinct set of beamformers in the spatial domain are probed. Second, the repetition leads to an increase of receive power by N/K^{FDB}.

Starting from here, the best beamformer can be found by projecting the receive signal $\mathbf{y}^{FDB}$ onto the orthogonal

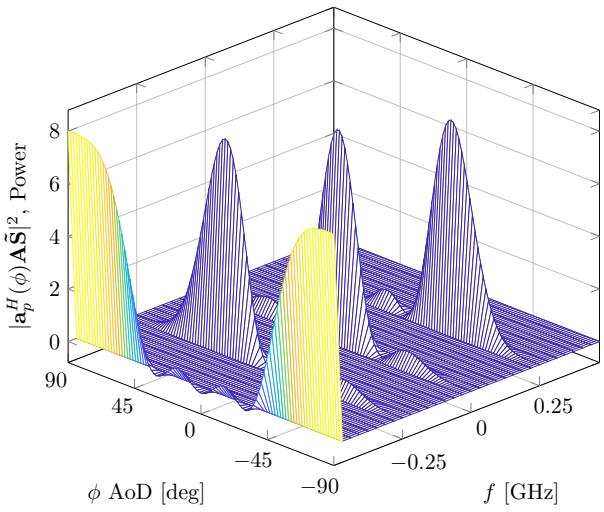

Fig. 2: (Virtual) codebook of beam patterns using FDB for $M = 4$, $K^{FDB} = 4$, $f_c = 100\,\text{GHz}$, and $f_b = 1\,\text{GHz}$ after receiving 8 times repeated pilot sequence $N = 32$ samples

beamforming codebook (5). This is done by first calculating the least-squares solution and power of the estimated values

$$\hat{\mathbf{x}}^{FDB} = \mathbf{y}^{FDB}\tilde{\mathbf{S}}^H\left(\tilde{\mathbf{S}}\tilde{\mathbf{S}}^H\right)^{-1}. \tag{28}$$

The entry in $\hat{\mathbf{x}}^{FDB}$ with maximum power, determines which beamformer from the orthogonal codebook should be chosen

$$\hat{q}_{max}^{FDB} = \arg\max \left|\hat{\mathbf{x}}^{FDB}\right|^2. \tag{29}$$

Again, if we replace the noisy samples in (28) with the noise-free receive signals, we obtain the optimal noise-free solution using the least-squares approach. Choosing the sampling points kf_s such that $\mathbf{A}$ matches $e^{-j2\pi\mathbf{F}_{TTD}^{orth}}$, the diagonal matrix $\mathbf{D}_l$ in (27) can be neglected for a single path channel as we are only interested in the absolute values. However, for multi-path scenarios with a significant second (or even third) scattering cluster in the environment, this least-squares detection method could lead to ambiguities and wrong decisions for the optimal beam. The phase term entries in $\mathbf{D}_l$ and large α_l lead to constructive or destructive superposition in $\hat{\mathbf{x}}^{FDB}$ by summation of all paths l where the delays of the paths are counted modulo K^{FDB}. In the simulation results in Sec. V, a closer look is taken at this problem.

The estimated index $\hat{q}_{max}^{FDB}$ of the best beam is used to evaluate $\bar{l}$ for frequency dependent beamforming and by updating the nominator in (22), we obtain a performance measure for this scheme.

IV. Beam Alignment - Variable Length Testing

The benefits of variable length testing are mainly given by the possibility to adapt to varying channel conditions and stopping early on favorable SNR conditions. On average, less samples are needed to achieve similar error criterion or relative power losses $\bar{l}$ [3].

A. Exhaustive Search

Based on (20), we can define a variable length testing scheme closely following [16]. For this, we multiply the receive vector $\mathbf{y}_q^{ES} = [y_q^{ES}[0], ..., y_q^{ES}[n-1]]$ with the conjugated complex pilot sequence $s^*[k]$ with all possible cyclical shifts $u \in [0, ...K^{ES}-1]$ of length n. For each shift u, we store the cross-correlation value in $\hat{\mathbf{x}}_q^{ES}$, which will be used to estimate the time-shift $\hat{u}$ by a simple max-comparison operation. Moreover, we are able to estimate the noise samples $\hat{z}$ and, thus, also the noise-variance $\hat{\sigma}_z^2$. The estimated maximum entry of $\hat{\mathbf{x}}_q^{ES}$ and the estimated noise variance $\hat{\sigma}_z^2$, defines a variable length generalized likelihood ratio test (GLRT) [16], [3]

$$\gamma_q[n] = n \log\left(1 + \frac{\left|\hat{\mathbf{x}}_q^{ES}[\hat{u}]\right|^2}{\hat{\sigma}_z^2}\right), \tag{30}$$

evaluated repeatedly for increasing sequence length n. For each beamformer $q \in |Q|$, we test $\gamma_q[n]$ against a termination threshold using the inequality $\gamma_q[n] \lesseqgtr \gamma_{term} = [Q^{-1}(\frac{P_{FA}}{2})]^2$, where P_{FA} has the meaning of a probability of false-alarm. The first beamformer $\hat{q}_{max}$ or hypothesis, which surpasses the threshold stops the test and is chosen as best estimated beamformer. This selected estimated beamformer is used to calculate the $\bar{l}$ value following (22).

B. Frequency Dependent Beamforming

In this section, we extend the approach given in [3]. Instead of estimating the noise variance and applying the GLRT as in [3], we apply the technique given in [17, Theorem 9.1]. The system model in (23) (or (27)), is a linear system model where $\mathbf{S}$ (or $\tilde{\mathbf{S}}$) is a known observation matrix and $\mathbf{Z}$ (or $\mathbf{z}$) a complex Gaussian noise vector with $\mathcal{CN}(0, \sigma_z^2\mathbf{I})$. We further define $\mathbf{y}_n^{FDB} = [y^{FDB}[0], ..., y^{FDB}[n-1]]$ and $\mathbf{G}_n = \tilde{\mathbf{S}}_n^H \tilde{\mathbf{S}}_n$, to derive an estimate at time instant n, $\hat{\mathbf{x}}_n^{FDB} = \mathbf{y}_n^{FDB}\tilde{\mathbf{S}}_n^H \left(\tilde{\mathbf{S}}_n \tilde{\mathbf{S}}_n^H\right)^{-1}$. All this allows us to adapt the GLRT for the classical linear model [17, Theorem 9.1], and a hypothesis testing problem is obtained from the metric

$$T_m(\mathbf{y}_n^{FDB}) = \frac{\left|\{\hat{\mathbf{x}}_n^{FDB}\right|^2\}_m^* \{\mathbf{G}_n^{-1}\}_{m,m} \left|\{\hat{\mathbf{x}}_n^{FDB}\right|^2\}_m}{\mathbf{y}_n^{FDB^H}\left(\mathbf{I} - \tilde{\mathbf{S}}_n \mathbf{G}_n^{-1} \tilde{\mathbf{S}}_n^H\right)\mathbf{y}_n^{FDB}}. \tag{31}$$

Its value is checked against a threshold using $(n-M)\,T_m(\mathbf{y}_n^{FDB}) \lesseqgtr \gamma^{FDB}[n]$. The length dependent threshold $\gamma^{FDB}[n] = \{Q_F\,(1-P_{FA}, n-M)\}^{-1}$ is defined as the inverse of an F distribution parameterized by the specified probability of false alarm P_{FA}, the current number of samples n, and the total number of beamformers M or hypotheses. The beamformer $\max_m (n-M)\,T_m(\mathbf{y}_n^{FDB})$ which surpasses $\gamma^{FDB}[n]$ first is selected. Following (22), we can derive the performance metric $\bar{l}$ for the frequency dependent variable length testing scheme. In contrast to [3], the results in (31) jointly calculate the decision criterion and take all the observations into account to estimate the threshold for each beamformer $T_m(\mathbf{y}_n^{FDB})$.

V. Simulation Results

Before we discuss the time efficiency of the proposed frequency dependent beamforming scheme, we need to define the simulation setup. The mmWave channel is assumed to be constant during the coherence time and each path is modeled by Rician fading [8] with path gain $\alpha_l \sim \sqrt{\rho_l}\left(\sqrt{\frac{\eta_l}{1+\eta_l}} + \frac{1}{\sqrt{1+\eta_l}}\epsilon_l\right)$, where η_l is the Rician coefficient and $\epsilon_l \sim \mathcal{CN}(0,1)$. We assume $L=3$ paths, where $(\rho_1 = 1, \eta_1 = 100)$,$(\rho_2 = 0.1, \eta_2 = 10)$, and $(\rho_3 = 0.1, \eta_3 = 0)$, which leads to a scenario where the dominant/line-of-sight path arrives with around 10 dB larger receive power at the UE. The AoD for each path is uniformly distributed as $\phi_l \sim U[-\frac{\pi}{2}, +\frac{\pi}{2}]$ as well as the time of flight being a continuous random variable $\tau_l \sim U\,[0, NT_s]$. In case τ_l is larger than the length of period of the pilot sequence, a modulo KT_s operation is used which maps back τ_l onto the periodic sequence length. For single-path evaluation, we simply ignore the contributions of α_2 and α_3. Furthermore, the antenna element distance is set to $d = \frac{c}{2f_c}$ for carrier frequency $f_c = 100\,\text{GHz}$ and a linear chirp signal with bandwidth $f_b = 1\,\text{GHz}$ is transmitted. We fix $K^{ES} = 50$, meaning that each beamformer in exhaustive search is tested with 50 training samples. This leads to a total of $N = MK^{ES}$ observations. Frequency dependent beamforming uses a pilot sequence length of $K^{FDB} = M$ and repeats the sequence N/K^{FDB} times. The SNR is defined as the expected value of the ratio of the receive power selecting the optimal analog beamformer q_{max} over the noise power.

For the evaluation of the variable length testing procedure, we design a linear chirp pilot sequence of length $K^{ES} = 255$ for ES which makes in total a maximum number of samples $N_{max} = MK^{ES}$ and for FDB we repeat a $K^{FDB} = M$ pilot sequence until N_{max} samples are obtained. However, the actual amount of observations N_{vl} is the expected value of the random variable $\mathrm{E}[n]$. Our stopping criterion is derived from the probability of false alarm set to $P_{FA} = 10^{-4}$ for ES and FDB achieving $\bar{l}$ values in the regime of 10^{-2} for SNR values around 0 dB and $L=1$. To obtain reliable noise variance estimates $\hat{\sigma_z}^2$ in (30), we allow a decision after receiving at least $N_{min} = 10$ samples in the ES case and after $K^{FDB} = M$ samples in the FDB case. Finding the set of parameters K^{ES}, P_{FA}, N_{max}, and N_{min} to achieve $\bar{l}$ values for ES and FDB variable length testing was done by a brute-force trial and error method.

Figure 3 depicts the performance of fixed length testing using a true time delay FDB in line of sight only with $L=1$ and for multi path with $L=3$. For $L=1$, FDB outperforms ES w.r.t. $\bar{l}$ values over the complete SNR domain as well as for $L=3$ below SNR of 1 dB. From Fig. 3, we can derive the previously mentioned detrimental effect of FDB performance in multi-path scenarios $L=3$. As we test with a regular ULA, the beamwidth is defined by the number of its antenna elements M. The likelihood of addressing more than one scatterer for wider beamwidth is increased and, thus, destructive interference in the receive power spectrum may occur more often. Moreover, the FDB scheme uses a repeated pilot sequence of length $K^{FDB} = M$. Because of that, M dictates how many different path delays can be resolved in the discrete time domain, where larger M leads

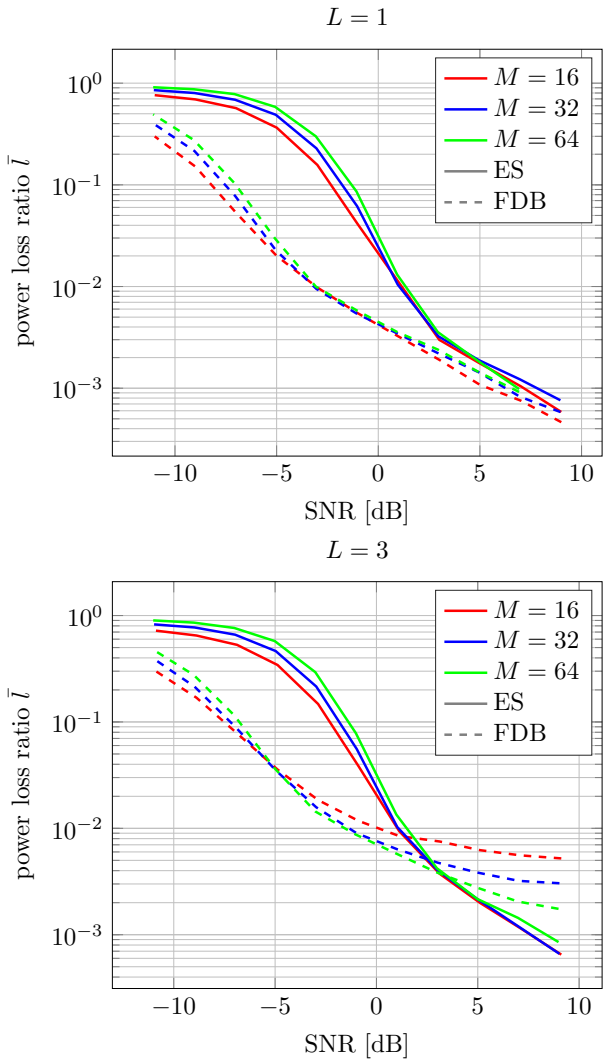

Fig. 3: Comparison of ES and FDB: $\bar{l}$ as function of SNR for fixed length test; above single path $L = 1$ and below multi path $L = 3$ for $f_c = 100\,\text{GHz}$, $f_b = 1\,\text{GHz}$, and $K^{ES} = 50$ with $N = MK^{ES}$ total number of observation for $M = [16, 32, 64]$

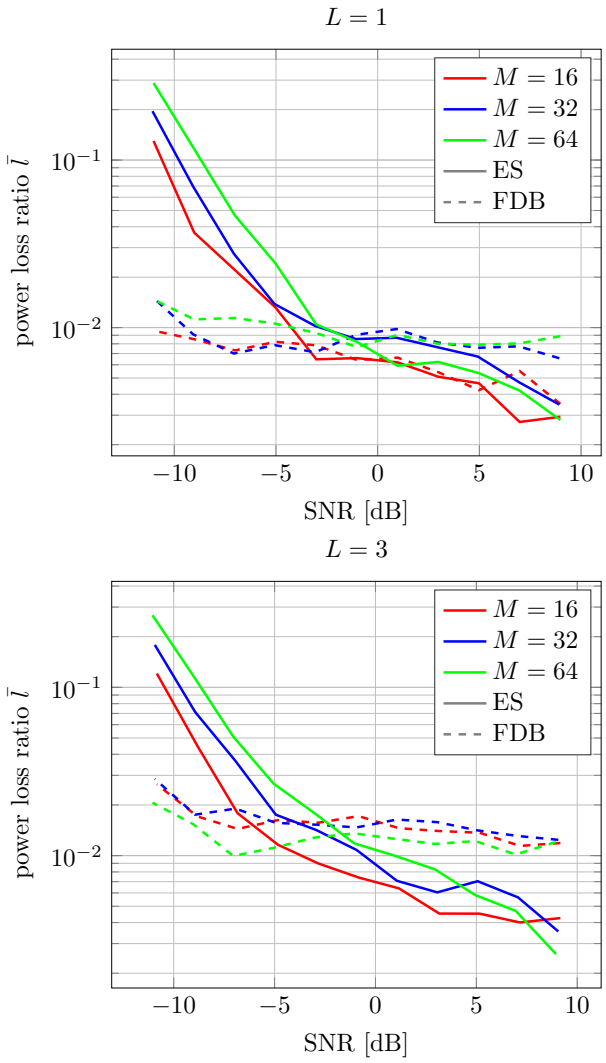

Fig. 4: Comparison of ES and FDB: $\bar{l}$ as function of SNR for variable length test; above single path $L = 1$ and below multi path $L = 3$ for $f_c = 100\,\text{GHz}$, $f_b = 1\,\text{GHz}$, and $N_{max} = 255$ for $M = [16, 32, 64]$

to less timing collisions within the periodically repeated receive sequence. So by increasing the number of antenna elements M, smaller $\bar{l}$ can be achieved and eventually the performance gap to the ES scheme or single-path case $L = 1$ is closed.

In Fig. 4 and Fig. 5, we present the results for the variable length test parameterized by $P_{FA} = 10^{-4}$ and $K^{ES} = 255$ achieving $\bar{l}$ of approximately 10^{-2}. We can derive that FDB achieves the targeted $\bar{l}$ over a wide SNR range, whereas ES violates it in the lower regime for $SNR \leq -5$ dB but slightly overperforms in the higher SNR regime. Larger $\bar{l}$ values at low SNR can be explained as $N_{max} = 255$ per beamformer samples are not sufficient to detect the optimal beam. As the parameters P_{FA} and K^{ES} are defined to achieve an $\bar{l} \approx 10^{-2}$ at around 0 dB, these adversarial effects in higher SNR and lower SNR regime need to happen. Adaptivity over a wider range of SNR is therefore only achieved by using FDB over ES [16], as every sample collected at the receiver helps detecting the correct beamformer. Lastly, from Fig. 5, we present the number of samples to achieve $\bar{l}$ in Fig. 3 and Fig. 4. With this, the following two observations can be made: First, variable length testing outperforms fixed length testing, especially in the higher SNR regime in terms of $\bar{l}$ using minimum amount of observations. Second, FDB hereby can further improve the time efficiency in combination with variable length testing. For example, at SNR ≈ 5 dB, we obtain equal $\bar{l}$ values for $L = 1$, but FDB needs less than half of the samples. Summing up, whenever we can expect to operate in scenarios with a dominant LOS path, the FDB method may be preferred over ES.

VI. Conclusion

In this work, we describe frequency dependent beamforming and its time-efficiency w.r.t. exhaustive search for testing an orthogonal codebook. The proposed beamforming technique assume a BS operating in downlink beam training without

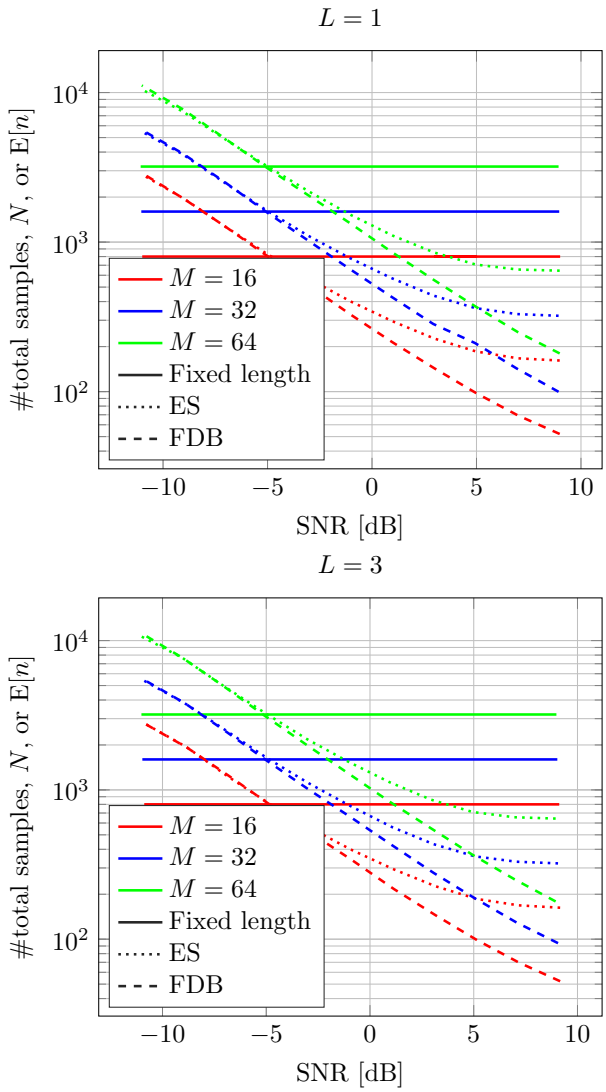

Fig. 5: Comparison of ES and FDB: number of expected variable length E[n] and fixed length observations N with $f_c = 100\,\text{GHz}$, $f_b = 1\,\text{GHz}$, $N_{max} = 255$ and $K^{ES} = 50$ for $M = [16, 32, 64]$

any prior time/frame synchronization. All UEs are able to listen to such a repeated broadcast pilot signal and decide on a favorable beamformer from a given analog codebook solely based on the receive spectrum. In general, this scheme performs best in sparse scattering environments which occur in mmWave communications.

For single-path scenarios, FDB outperforms the brute foce method of exhaustive search over the complete SNR range for fixed as well as variable length tests. For multi-path scenarios, FDB may suffer due to the superposition of all paths in the spectrum leading to constructive and/or destructive interference. This effect is negatively correlated to the beamwidth of the beamformers under test and therefore depends on the number of antenna elements of the ULA. However, for both scenarios, multi-path and single-path, in medium and high SNR, power loss measures $\bar{l} \approx 10^{-2}$ can be achieved. As this comparison neglects extensive scheduling/orchestration of several UEs for the reference scheme of exhaustive search, we can safely promote using FDB at BSs to speed-up the beam alignment in mmWave communication. The additional hardware expense for a passive true time delay network, which is capable of producing a frequency/angular sweep implemented by time delays that are multiples of the Nyquist sampling interval, is negligible in comparison to the ease of orchestrating several UEs in field and testing all beamformers simultaneously. Still, further investigations are needed to improve time-efficiency and to reduce the expected relative power losses in presence of strong multi-path or pure non-line of sight conditions.

Acknowledgment

We would like to thank Fabian Diehm for valuable comments and fruitful discussions. This work has been supported by the German Research Foundation (DFG) within the project ”AgileHyBeams” and by the German Federal Ministry of Education and Research (BMBF) within the project ”Landnetz”.

References

[1] V. Va and R. W. Heath, “Basic relationship between channel coherence time and beamwidth in vehicular channels,” in *2015 IEEE 82nd Vehicular Technology Conference (VTC2015-Fall)*, 2015, pp. 1–5.

[2] A.-A. A. Boulogeorgos, A. Alexiou *et al.*, “Terahertz technologies to deliver optical network quality of experience in wireless systems beyond 5G,” *IEEE Commun. Mag.*, vol. 56, no. 6, pp. 144–151, 2018.

[3] M. Khalili Marandi, C. Jans *et al.*, “Evaluation of detection accuracy and efficiency of considered beam alignment strategies for mmwave massive mimo systems,” in *Proc. Asilomar Conf. Signals Syst. Comput*, 2021, pp. 664–671.

[4] C. Jeong, J. Park, and H. Yu, “Random access in millimeter-wave beamforming cellular networks: issues and approaches,” *IEEE Commun. Mag.*, vol. 53, no. 1, pp. 180–185, 2015.

[5] A. F. Molisch, V. V. Ratnam *et al.*, “Hybrid Beamforming for Massive MIMO: A Survey,” *IEEE Commun. Mag.*, vol. 55, no. 9, pp. 134–141, Sep. 2017.

[6] M. Danielsen and R. Jorgensen, “Frequency scanning microstrip antennas,” *IEEE Trans. Antennas Propag.*, vol. 27, no. 2, pp. 146–150, March 1979.

[7] C. Jans, X. Song *et al.*, “Frequency-selective analog beam probing for millimeter wave communication systems,” in *Proc. IEEE Wireless Commun. Netw. Conf.*, 2020, pp. 1–6.

[8] X. Song, S. Haghighatshoar, and G. Caire, “Efficient beam alignment for millimeter wave single-carrier systems with hybrid mimo transceivers,” *IEEE Trans. Wireless Commun.*, vol. 18, no. 3, pp. 1518–1533, 2019.

[9] A. Wadaskar, V. Boljanovic *et al.*, “3D rainbow beam design for fast beam training with true-time-delay arrays in wideband millimeter-wave systems,” in *Proc. Asilomar Conf. Signals Syst. Comput*, 2021, pp. 85–92.

[10] R. Rotman, M. Tur, and L. Yaron, “True time delay in phased arrays,” *Proc. of the IEEE*, vol. 104, no. 3, pp. 504–518, 2016.

[11] J. Butler, “Beam-forming matrix simplifies design of electronically scanned antennas,” *Electronic Design*, vol. 9, pp. 170–173, 1961.

[12] D. I. Lialios, N. Ntetsikas *et al.*, “Design of true time delay millimeter wave beamformers for 5G multibeam phased arrays,” *Electronics*, vol. 9, no. 8, 2020.

[13] B. Wang, F. Gao *et al.*, “Spatial- and Frequency-Wideband Effects in Millimeter-Wave Massive MIMO Systems,” *IEEE Trans. Signal Process.*, vol. 66, no. 13, pp. 3393–3406, Jul. 2018.

[14] C. Jans, X. Song *et al.*, “Fast beam alignment through simultaneous beam steering and power spectrum estimation using a frequency scanning array,” in *24th International ITG Workshop on Smart Antennas*, 2020, pp. 1–6.

[15] W. Rave and C. Jans, “On the Mapping between Steering Direction and Frequency of a Uniform Linear Array with Fixed True Time Delays,” in *24rd International ITG Workshop on Smart Antennas*, Feb. 2020, pp. 1–6.

[16] M. K. Marandi, W. Rave, and G. Fettweis, “Beam selection based on sequential competition,” *IEEE Signal Process. Lett.*, vol. 26, no. 3, pp. 455–459, 2019.

[17] S. Kay, *Fundamentals of Statistical Signal Processing, vol. II: Detection Theory*. Prentice Hall, 1998.